Synthesis, molecular docking, bio-evaluation and quantitative structure activity relationship of new chalcone derivatives as antioxidants

Siddiqa, Aysha; Tajammal, Affifa ; Irfan, Ahmad; Azam, Muhammad; Munawar, Munawar Ali; Hardy, Rowan S; Asim Raza Basra, Muhammad

DOI:
10.1016/j.molstruc.2022.134814

Synthesis, molecular docking, bio-evaluation and quantitative structure activity relationship of new chalcone derivatives as antioxidants

Aysha Siddiqa[a], Affifa Tajammal[a,b], Ahmad Irfan[c,d], Muhammad Azam[e], Munawar Ali Munawar[f], Rowan Hardy[g], Muhammad Asim Raza Basra[a*]

Aysha Siddiqa
ayeshasiddiqaphd@gmail.com

Affifa Tajammal
affifa.tajammal@lgu.edu.pk

Ahmad Irfan
irfaahmad@gmail.com

Muhammad Azam
azammuhammad.chem@pu.edu.pk

Munawar Ali Munawar
mamunawar.chem@pu.edu.pk

Rowan Hardy
r.hardy@bham.ac.uk

Muhammad Asim Raza Basra*
asimbasra.chem@pu.edu.pk
asimarbasra@gmail.com

[a] Centre for Clinical and Nutritional Chemistry, School of Chemistry, University of the Punjab, New Campus, Lahore, Pakistan

[b]Department of Chemistry, Lahore Garrison University, Lahore, Pakistan

[c]Research Center for Advanced Materials Science (RCAMS), King Khalid University, P.O. Box 9004, Abha 61413, Saudi Arabia

[d]Department of Chemistry, College of Science, King Khalid University, P.O. Box 9004, Abha 61413, Saudi Arabia

[e]Centre for Applied Chemistry, School of Chemistry, University of the Punjab, New Campus, Lahore, Pakistan

[f]Department of Chemistry, faculty of Sciences, University of Central Punjab, Lahore, Pakistan

[g]Institute of Clinical Sciences, University of Birmingham, UK

Highlights

- 2-Hydroxy-5-nitro-chalcones (3a-3e) were synthesized and characterized by spectroscopic studies.
- Antioxidant potential was determined by DPPH and iron chelation.
- Computational studies were performed using DFT approach and molecular docking was performed against Keap1.
- Furthermore *in vivo* study was performed to investigate analgesic and anti-inflammatory potential.

Abstract

The therapeutic suppression of oxidative stress represents an attractive therapeutic target across an array of inflammatory disease setting. The nuclear factor erythroid 2–related factor 2 (Nrf2) and its negative regulator Kelch-like ECH-associated protein1 (Keap1) are principal components in the homeostatic regulatory responses to oxidative and electrophilic stress and as such, reflect promising therapeutic targets. Flavonoids are a structurally diverse class of compounds possessing a wide range of pharmacological properties that have been postulated to suppress inflammation through their suppression of the Nrf2 pathway. The present study describes the synthesis of new 2-Hydroxy-5-nitro chalcones in the flavonoid family by the condensation of acetophenone and benzaldehydes. The structures of these compounds (**3a-3e**) were elucidated by spectroscopic studies including FTIR, ^{1}H NMR and ^{13}C NMR. Antioxidant potential of the compounds was determined by DPPH and iron chelating assays. Molecular docking analysis revealed that all the compounds had a marked affinity for Keap1 and computational studies revealed that all compounds possessed antioxidant potential. The compounds **3a**>**3b**>**3c**>**3e**>**3d** showed an increasing order in IC_{50} for iron chelation, but were poor DPPH scavengers. Anti-inflammatory

and analgesic activities were determined by carrageenan induced paw edema and acetic acid induced writhing test respectively in Sprague–Dawley rats. Of the compounds studied, both **3a** and **3b** demonstrated significant anti-inflammatory properties while **3c** possessed analgesic effects. These studies suggest that these new 2-Hydroxy-5-nitro chalcones are potential anti-oxidant and anti-inflammatory compounds through their interaction with the Nrf2-Keap1 pathway. Further study of these compounds at the molecular level is now required to validate the presence of Nrf2 dependent anti-inflammatory pathway.

Keywords: Chalcones, Antioxidants, Anti-inflammatory, Nrf2, QSAR

1. Introduction

Chronic inflammation contributes to the pathophysiology age related diseases such as arteriosclerosis, insulin resistance and cardiovascular diseases [1-4]. Oxidative stress and damage driven by free radicals play a central role in both driving and mediating the deleterious actions of chronic inflammation [5].

The nuclear factor-erythroid factor 2-related factor 2 (Nrf2), and its negative regulation by Kelch-like ECH-associated protein 1(Keap1), is a master regulator of the antioxidant response and suppression of oxidative stress in response to inflammation [6]. Its contributions to the suppression of oxidative stress are driven by orchestrating the recruitment of inflammatory cells and regulating antioxidant and anti-inflammatory gene expression via Nrf2/Keap1/ARE pathway. The therapeutic targeting of the Nrf2/Keap1/ARE pathway represents a novel way in which to suppress inflammation in human disease, with a reduced side effect profile [7, 8].

Chalcones are flavonoid-type phenolic compounds that are biosynthesized via the shikimate pathway and are sometimes referred to as "open chain flavonoids". Chalcones are favored in medicinal chemistry due to their relative ease of production and modification, which reflects the ease with which they are formed in nature[9]. Current chalcone synthetic methodologies are generated through the use of an alkaline base and a polar solvent to link two aromatic molecules, such as acetophenone and benzaldehyde, to generate the core chalcone nucleus [10].

The presence of α,β-unsaturated carbonyl system in chalcone derivatives contribute to a wide array of reported biological properties including antioxidant/inflammatory action [11], anticancer [12], antibacterial [13], antimalarial [14], anti-HIV [15], anti-leishmanial [16], and neuroprotective properties [17]. Their mechanisms of action are diverse, are reported to include the inhibition of

pro-inflammatory mediators like prostaglandin E2, and suppression of the inflammatory COX2, inducible NO synthase and NFkβ inflammatory pathways [11, 14]. In addition, a central mechanism of their action has been proposed to be the upregulation of Nrf2, either directly, or through the inhibition of Keap1 to ameliorate oxidative stress and restore redox homeostasis [18, 19]. In this study we describe the *in vitro*, *in silico*, *in vivo* and computational investigations of newly synthesized chalcone derivatives.

2. Experimental

2.1. Chemistry

The progress of reaction was observed by silica gel 60 F254 TLC plates and spots were visualized under UV radiation. FTIR spectra were recorded on Agilent Technologies 41630. The ^{1}H NMR and ^{13}C NMR spectra were recorded on AVANCE AV- 400 MHz and AVANCE AV-500 MHz, Bruker 125 MHz respectively. While EIMS data were recorded on JEOL MS 600H-1.

2.2. General method for the synthesis of 2-Hydroxy-4-nitro chalcones (3a-3e)

To a stirred solution of 2-Hydroxy-5-nitroacetophenone (6 mmol) and aromatic benzaldehyde (6 mmol) in 25 ml ethanol, KOH (20 % w/v aqueous solution, 6 mL) was added and the mixture was stirred at room temperature for 24–36 h. The progress of reaction was monitored by performing TLC using hexanes: ethyl acetate (7:3). The reaction mixture was cooled to ^{0}C (ice-water bath) and acidified with HCl (10 % v/v aqueous solution). The product was recrystallized with ethanol to obtain **3a** to **3e**.

2.3. (E)-3-(4-Fluorophenyl)-1-(2-Hydroxy-5-nitrophenyl) prop-2-en-1-one (3a)

Appearance: Yellow needles; Yield: 1.2 g (70 %) Melting Point: 233 °C, FT-IR: υ (cm^{-1}): 3267 (-OH), 3098 (=C-H), 1642 (C=O), 1506, 1473 (C=C), 1565, 1348 (-NO_2), 1192 (C-F). ^{1}H NMR:

(500 MHz / DMSO-d_6): δ 12.76 (1H, s, 2′-OH), 8.76 (1H, s, 6′-H), 8.36 (1H, d, J = 8.8 Hz, 4′-H), 7.98 (2H, bs, 2-H, 6-H), 7.87-7.78 (2H, m, α-H, β-H), 7.35-7.31 (2H, m, 3-H, 5-H), 7.21 (1H, d, J = 9.0 Hz, 3′-H). ^{13}C NMR: (125 MHz / DMSO-d_6): δ 191.96 (C=O), 165.27(2′-C), 163.18 (4-C), 144.52 (β-C), 132.11 ($^{m}J_{C-F}$ = 8.8 Hz, 2-C, 6-C), 131.52 ($^{p}J_{C-F}$ = 2.5 Hz, 1-C), 130.19 (4′-C), 127.09 (6′-C), 123.86 (1′-C), 123.67 (3′-C), 118.99 (α-C), 116.56 ($^{o}J_{C-F}$ = 21.6 Hz, 3-C, 5-C).

2.4. (E)-3-(4-Chlorophenyl)-1-(2-Hydroxy-5-nitrophenyl) prop-2-en-1-one (3b)

Appearance: Yellow needles, Yield: 1.3 g (72 %), Melting Point: 231 °C, FT-IR: υ (cm^{-1}): 3257 (-OH), 3123 (=C-H), 1649 (C=O), 1523, 1464 (C=C), 1565, 1363 (-NO_2), 635 (C-Cl). ^{1}H NMR:(500 MHz / DMSO-d_6): δ 12.75 (1H, s, 2′-OH), 8.74 (1H, s, 6′-H), 8.35 (1H, d, J = 9.0 Hz, 4′-H), 7.92-7.89 (3H, m, α-H, 2-H, 6-H), 7.77 (1H, d, J = 15.6 Hz, β-H), 7.55-7.53 (2H, m, 3-H, 5-H), 7.19(1H, d, J = 9.0 Hz, 3′-H). ^{13}C NMR: (125 MHz / DMSO-d_6): δ 191.83 (C=O), 165.26 (2′-C), 144.09 (β-C),140.10 (5′-C), 136.07 (4-C), 133.78 (1-C), 131.30 (2-C, 6-C), 130.20 (4′-C), 129.53 (3-C, 5-C), 127.14 (6′-C), 124.71 (1′-C), 123.64 (3′-C), 119.00 (α-C).

2.5. (E)-3-(4-Bromophenyl)-1-(2-Hydroxy-5-nitrophenyl) prop-2-en-1-one (3c)

Appearance: Yellow needles, Yield: 1.5 g (71 %), Melting Point: 235 °C, FT-IR: υ (cm^{-1}): 3302 (-OH), 3092 (=C-H), 1673 (C=O), 1562, 1432 (C=C), 1535, 1356 (-NO_2), 554 (C-Br). ^{1}H NMR:(500 MHz / DMSO-d_6): δ 12.71 (1H, s, 2′-OH), 8.74 (1H, s, 6′-H), 8.36 (1H, d, J = 9.0 Hz, 4′-H), 7.91 (1H, d, J = 15.6 Hz, α-H), 7.85 (2H, d, J = 7.8 Hz, 2-H, 6-H), 7.76 (1H, d, J = 15.6 Hz, β-H), 7.69 (2H, d, J = 7.9 Hz, 3-H, 5-H), 7.20(1H, d, J = 9.1 Hz, 3′-H). ^{13}C NMR: (125 MHz / DMSO-d_6): δ 191.19 (C=O), 165.19 (2′-C), 144.16 (β-C), 140.07 (5′-C), 134.13 (1-C), 132.48 (3-C, 5-C), 131.49 (2-C, 6-C), 130.19 (4′-C), 127.14 (6′-C), 124.99 (1′-C), 124.88 (3′-C), 123.78 (4-C), 119.00 (α -C).

2.6. (E)-1-(2-Hydroxy-5-nitrophenyl)-3-(3-nitrophenyl) prop-2-en-1-one (3d)

Appearance: orangish yellow needles, Yield: 1.1 g (58 %), Melting Point: 217 °C, FT-IR: υ (cm^{-1}): 3316 (-OH), 3102 (=C-H), 1651 (C=O), 1502, 1467 (C=C), 1545, 1326 ($-NO_2$), ^{1}H NMR: (500 MHz / DMSO-d_6): δ 12.70 (1H, s, 2′-OH), 8.74 (1H, s, 2-H), 8.36 (1H, d, *J* = 9.1 Hz, 4′-H), 8.15 (1H, s, 6′-H), 7.93 (1H, d, *J* = 15.7 Hz, α-H), 7.88 (1H, d, *J* = 7.6 Hz, 4-H), 7.75 (1H, d, *J* = 15.7 Hz, β-H), 7.67 (2H, d, *J* = 7.8 Hz, 6-H), 7.44 (1H, d, *J* = 7.8 Hz, 5-H),7.20 (1H, d, *J* = 9.1 Hz, 3′-H).^{13}C NMR: (125 MHz / DMSO-d_6): δ 191.88 (C=O), 165.20 (2′-C), 143.72 (3-C), 140.09 (5′-C), 137.33 (β-C), 133.94 (1-C), 131.74 (6-C), 131.52 (4′-C), 130.25 (5-C), 128.69 (6′-C), 127.16 (4-C), 125.58 (2-C), 123.67 (1′-C), 122.88 (3′-C), 118.99 (α -C).

2.7. (E)-1-(2-Hydroxy-5-nitrophenyl)-3-(4-methoxyphenyl) prop-2-en-1-one (3e)

Appearance: light yellow colored needles, Yield: 1.1 g (61 %), Melting Point: 203 °C FT-IR: υ (cm^{-1}): 3570 (-OH), 3081 (=C-H), 1635 (C=O), 1558, 1472 (C=C), 1550, 1341 ($-NO_2$).^{1}H NMR (500 MHz / DMSO-d_6): δ 12.95 (1H, s, 2′-OH), 8.79 (1H, s, 6′-H), 8.36 (1H, d, *J* = 9.1 Hz, 4′-H), 7.88 (2H, d, *J* = 7.9 Hz, 2-H, 6-H), 7.80 (2H, s, α-H, β-H), 7.19 (1H, d, *J* = 9.1 Hz, 3′-H), 7.05 (2H, d, *J* = 7.9 Hz, 3-H, 5-H) ^{13}C NMR: (125 MHz / DMSO-d_6): δ 192.08 (C=O), 165.54 (2′-C), 162.38 (4-C), 146.26 (β-C), 140.08 (5′-C), 131.84 (2-C, 6-C), 130.13 (4′-C), 127.44 (1-C), 127.02 (6′-C), 123.39 (1′-C), 120.99 (3′-C), 119.02 (α -C), 115.03 (3-C, 5-C), 55.94 (O***C***H_3).

2.8 In vitro antioxidant activities

The *in vitro* antioxidant potential of the synthesized compounds was evaluated by two different assays i-e DPPH free radical scavenging assay and iron chelating activity as reported earlier [20], [21].

2.9. In silico studies

Molecular docking of all the synthesized compounds was performed against Keap1 retrieving the 3D crystal structure of the Keap1 (PDB ID: 2FLU at 1.50 Å resolution) protein from the Research Collaboratory for Structural Bioinformatics (RCSB) Protein Data Bank (PDB).

2.9.1. Preparation of target Keap1 and compounds for docking

The receptor protein was prepared for docking by eliminating water molecules and adding hydrogen atoms using the Discovery Studio (DS) 4.5 Visualizer. Avogadro software was used to create and optimize the 3D structures of the synthesized molecules. The PDB file format was used to receptor protein and synthesized chemicals [22].

2.9.2. Receptor-ligand interaction

Using Patch Dock, which utilizes the shape complementarity principles, the synthesized compounds were docked separately against Keap1[23]. In light of the amino acid residues in the binding pocket, the docking results were chosen. Atomic contact energy (ACE) and docking score were used to analyze the receptor-ligand interaction. Using Discovery Studio 4.5 Visualizer, interactions like hydrogen bonds and hydrophobic interactions were additionally captured around the binding pocket.

2.10. In vivo study

Sprague–Dawley (SD) rats (10-12 weeks old, 150-200g) were used for the experiments. The animals were kept under controlled conditions of temperature (25 ± 5°C) and humidity (50 ± 10%) according to the international ethical guidelines for the care of laboratory animals. Experiments were approved by Institutional Ethical Committee, University of the Punjab, Lahore (Approval No. D/025/2018, March 07, 2018).

2.11. Anti-inflammatory activity

Carrageenan-induced rat paw edema method was used to investigate the anti-inflammatory activity of the synthesized chalcones [24]. Rats were divided into three groups (n=6); carrageenan (carr),

standard diclofenac sodium (DS) and chalcones test groups. Both standard and test groups were given 20 mg/kg b.w. of DS and test compounds respectively emulsified with CMC (1%) via intragastric gavage. Carr group received only 1 % CMC. One hour after the drug administration, rats were induced with carrageenan (1%) in the sub planer surface of the hind right paws. Left hind paws were observed as control. To observe the effect of test compounds, paw volume of rats was measured after 1, 2, 3, and 4 hours of carrageenan injection. Percentage inhibition in paw edema was calculated by the following formula.

% edema inhibition = (Vc–Vt/Vc) × 100

Where Vc is mean paw volume (cm^3) of control group and Vt is mean paw volume (cm^3) of tested drug.

2.12. Analgesic activity

Previously reported acetic acid induced writhing test with some modifications was conducted to explore the analgesic effect of the tested chalcones. Rats were pre-treated with chalcones (20 mg/kg b.w.) and standard drug (20 mg/kg b.w.) orally followed by acetic acid (0.6 %) i.p. injection (10 ml/kg b.w.) after 1 hour. Control group was attended with vehicle only. The number of writhings and lickings were counted after 5 min of acetic acid injection for 25 minutes [25]. %inhibition in writhing/ licking was calculated by using the following formula:

$$\% \text{ Inhibition} = \frac{\text{Mean writhing/licking control} - \text{mean writhing/licking test}}{\text{mean writhing control}} \times 100$$

2.13. Computational detail

Previously published methodology was used for density functional theory (DFT) studies. Briefly, it is common to employ one-electron transfer and H-atom transfer processes to comprehend the radical scavenging process [26, 27]. We have clarified the one-electron transfer mechanism in the current work. Recently, it has been demonstrated that DFT studies of the compounds is an effective strategy for reproducing experimental data [28-30]. The B3LYP functional and 6-31G** basis set [31, 32] were used to optimize the ground state geometry. Previously published method was used to calculate the ionization potentials (IP), which were appended below [33].

$IP = -E_{HOMO}$ (1)

$EA = -E_{LUMO}$ (2)

All calculations were performed by Spartan '14 v1.1.8' at B3LYP/6-31G** level which has been proved an efficient and reasonable approach to shed light on the structure-activity relationship and other physiochemical properties [34, 35].

3. Results and discussion

Chalcones were synthesized by reacting 2-Hydroxy-5-nitroacetophenone (**1**) with different aromatic aldehydes in the presence of KOH by using Claisen-Schmidt condensation reaction (Scheme 1). The synthesized chalcones were obtained in higher yields (58-72%). All the prepared compounds have been characterized by infrared (IR), ^{1}HNMR and ^{13}CNMR. In IR spectra of synthesized chalcones, the α, β-unsaturated carbonyl group appeared in the range of 1635-1673 cm^{-1}. The two aromatic C=C stretching frequencies bands were observed in the range of 1432-1562 cm^{-1}. The C-F stretching frequency in compound **3a** was observed at 1192 cm^{-1}. C-Cl stretching in compound **3b** was noted at 635 cm^{-1}. C-Br stretching in compound **3c** was observed at 554 cm^{-1}. The NO_2 functional group showed two stretching frequency bands in the range of 1326-1565 cm^{-1} for compound **3d**. In ^{1}H NMR data of the compounds **3a-3e,** the signal in the range of δ12.71 - δ12.95 indicates the presence of 2′-OH. The signal in the reign of δ7.75 – δ7.93 indicated the presence of α-H and β-H. The coupling constant value of 15 Hz is a clear indication that the chalcones are present in trans form. The other aromatic protons also appeared at their respective regions. The physiochemical data of the synthesized compounds is summarized in Table 1.

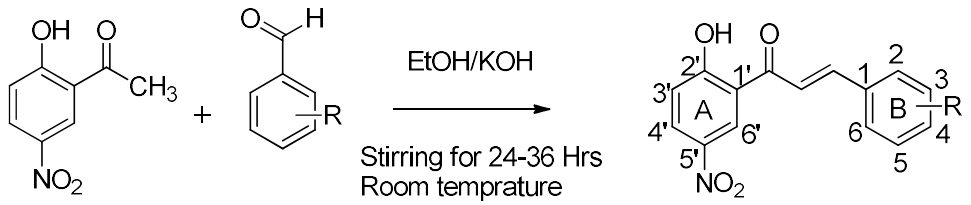

(1) (2)

R= 4-F, 4-Cl, 4-Br.
3-NO_2, 4-OCH_3

(3a), R= 4-F
(3b), R= 4-Cl
(3c), R= 4-Br
(3d), R= 3-NO_2
(3e), R= 4-OCH_3

Scheme 1: Scheme for the synthesis of 2-Hydroxy-5-nitro chalcones

Table 1: Physicochemical characterization data of the synthesized compounds

Compound	-R	Molecular Formula	Molecular weight	Melting point (°C)	Yield (%)
3a	4-F	$C_{15}H_{10}FNO_4$	287.24	233	70
3b	4-Cl	$C_{15}H_{10}ClNO_4$	303.03	231	72
3c	4-Br	$C_{15}H_{10}BrNO_4$	346.98	235	71
3d	3-NO_2	$C_{15}H_{10}N_2O_6$	314.05	217	58
3e	4-OCH_3	$C_{16}H_{13}NO_5$	299.28	203	61

3.1.In vitro antioxidant activities

Antioxidant potential of the synthesized chalcones was determined by the DPPH radical scavenging assay and iron chelating assay while trolox and ascorbic acid were used as standard antioxidants. DPPH activity of 2-Hydroxy-5-nitrochalcones showed that these chalcone are poor DPPH radical scavengers as their IC_{50} value is greater than 2000 μM (Table 2).

Table 2: IC_{50} (μM) for DPPH activity of 2-Hydroxy-5-nitro chalcones

Compounds	Time (Minutes)				
	15	**30**	**45**	**60**	**120**
Trolox	225.1±15.1	216.2±10.4	223.1±15.0	214.8±10.4	252.7±17.2
Ascorbic acid	215.5±10.4	221.3±14.8	234.4±15.7	244.4±15.9	240.4±15.8
3a	>2000	>2000	>2000	>2000	>2000
3b	>2000	>2000	>2000	>2000	>2000
3c	>2000	>2000	>2000	>2000	>2000
3d	>2000	>2000	>2000	>2000	>2000
3e	>2000	>2000	>2000	>2000	>2000

IC_{50} values for iron chelating activity of chalcones are presented in table 3. Chalcone **3a** has shown highest chelating activity as compared to other chalcones but less active than standards. The order of chelating activity for the chalcones was **3a**>**3b**>**3c**>**3e**>**3d** after 120 minutes of incubation.

Table 3: IC_{50} (μM) for iron chelating activity of 2-Hydroxy-5-nitro chalcones

Compounds	Time (Minutes)				
	10	**30**	**45**	**60**	**120**
Trolox	0.5±0.2	0.5±0.3	0.5±0.3	0.4±0.2	0.2±0.1
Ascorbic acid	3.3±1.2	2.2±1.1	0.3±0.7	0.2±0.5	0.2±0.6
3a	12.3±2.3	13.6±6.5	14.2±8.9	15.1±9.2	13.2±12.5
3b	18.5±11.9	17.5±15.8	23.6±18.9	28.1±13.7	19.8±1.3
3c	45.2±4.8	49.3±8.5	54.2±9.5	51.3±8.3	49.1±17.7
3d	58.8±13.2	59.2±16.4	78.3±21.9	89.2±25.7	90.1±34.2
3e	93.2±25.4	78.3±21.6	93.7±17.5	89.2±31.2	78.1±16.2

3.2. In silico studies

Molecular docking study was performed to explore the binding interaction of the synthesized chalcones with the Keap1. The compounds which interrupt the interaction between Nrf2 and Keap1 by binding with Keap1 can result in translocation of Nrf2 in the nucleus, where it transcripts the antioxidant and anti-inflammatory genes to reduce oxidative stress [36]. Docking interactions were visualized using DS 4.5 Visualizer and their 2D and 3D structures were plotted. Ligand molecules interacted with protein encountering different type of bindings i-e conventional hydrogen bond, alkyl, Pi alkyl, Pi-donor hydrogen bond, carbon hydrogen bond and unfavorable bumps Fig.1 and Fig.S11-S16. Table 4 shows docking score, area, atomic contact energy (ACE) values, binding residues and type of interactions. It is evident that all the compounds scored higher compare to ascorbic acid and trolox. The compounds having high docking score and lower ACE values means stronger interaction with the receptor protein [23].

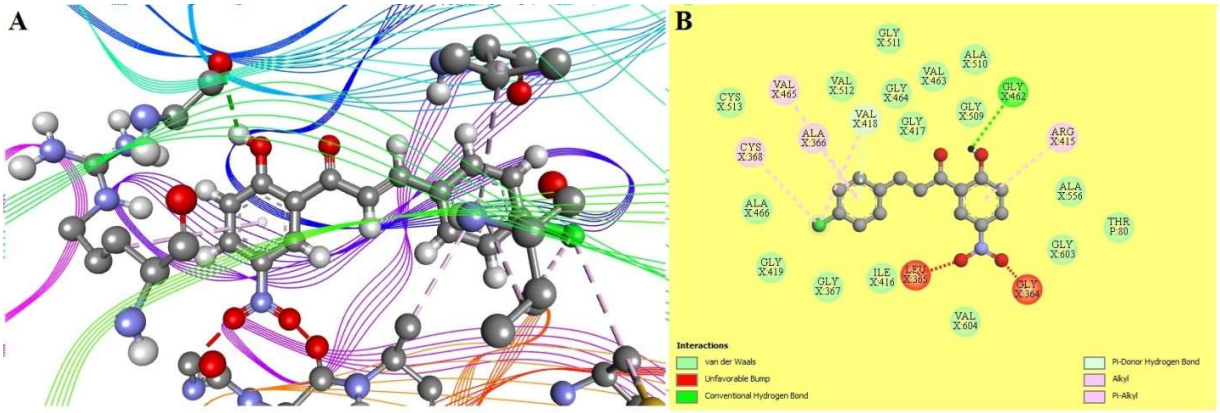

Figure 1: Illustration of 3D (A) and 2D (B) molecular interactions of **3b** with Keap1

Table 4: Molecular Docking study of chalcone derivatives against Keap1 (PDB ID: 2FLU)

Ligand	Docking score	Area	ACE	Interacting Residues	Interactions
3a	4372	474.3	-263.5	ILE 559, VAL 606, ARG 415 VAL 418, VAL 465	Conventional hydrogen bond Conventional hydrogen bond, unfavorable bump
3b	4822	593.5	-362.4	CYS 368 ARG 415, VAL 465, ALA 366 VAL 418 GLY 462 LEU 365, GLY 364	Alkyl Pi Alkyl Alkyl, Pi-donor hydrogen bond Conventional hydrogen bond Unfavorable bump
3c	4322	460.0	-283.5	CYS 513 LEU 365 GLY 605, ALA 366, GLY 509	Alkyl Unfavorable bump Carbon hydrogen bond
3d	4446	470.9	-319.5	GLY 364, GLY 464, GLY 603 ARG 415	Carbon hydrogen bond Pi Alkyl
3e	4500	469.1	-318.8	GLY 364, LEU 365 ALA 366, ARG 415, VAL 465 GLY 462 VAL 418	Unfavorable bump Pi Alkyl Conventional hydrogen bond Carbon hydrogen bond, Pi donor hydrogen bond
Ascorbic acid	2984	301.9	-143.2	ILE 416, LEU 557 GLY 464 ALA 510	Conventional hydrogen bond Van der waals Conventional hydrogen bond, Carbon hydrogen bond
Trolox	3934	425.30	-238.17	ALA 366 ARG 415 VAL 465, VAL 606	Alkyl, pi-alkyl Conventional hydrogen bond Alkyl

3.3. In vivo studies

Anti-inflammatory effect of synthesized chalcones was investigated by carrageenan induced paw edema in SD rats. Previous studies have reported that compounds possessing electron withdrawing groups at para-positions show evidence of anti-inflammatory properties [37]. The % inhibition of paw edema of test compounds and standard drug DS at dose 20 mg/kg has been depicted in Fig. 2. (A-B). It is evident that all the compounds inhibited paw edema from first hour of induction to fourth hour. Among all the compounds, **3a** and **3b** containing fluoro and chloro groups respectively at para position markedly inhibited paw edema at fourth hour of induction.

Analgesic activity of the test compounds was determined by acetic acid induced writhing test. The effect of the test compounds to subside pain induced by injecting acetic acid was observed by recording number of writhing and lickings and results were compared with DS as standard. (Table 5-6), (Fig. 2. C-D). The results exhibited that chalcone derivatives are moderate to considerable analgesics compared to DS. In this study compound **3c** was found to exhibit significant analgesic activity among all the synthesized compounds giving maximum reduction in the writhing (53.5%) and lickings (61.5%) in 25 minutes even greater than DS writhing (38.6%) and lickings (69.2%). While compound **3b** inhibited writhing (38.6%), equivalent to DS and lickings (19.2%).

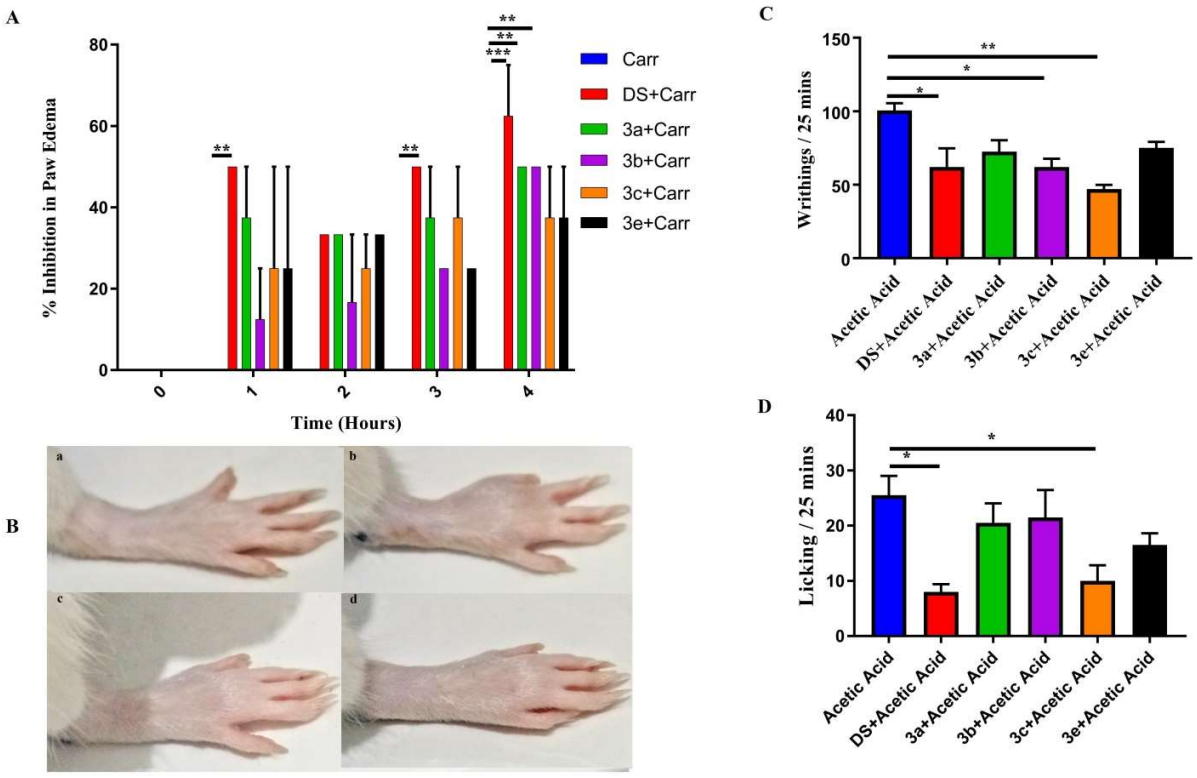

Figure 2: Anti-inflammatory and analgesic effect of chalcone derivatives in SD rats n=6. Percentage inhibition in carr induced paw edema at 1, 2, 3 and 4 hour of carr injection (A). Inflammatory response of (a) control, (b) carr, (c) carr + DS and carr + tested chalcones at 4th hour of carr injection (B). Effect of chalcone derivatives on the acetic acid induced writhing in 25 minutes after 5 minutes of 0.6% acetic acid injection (C). Effect of chalcones on acetic acid induced lickings in 25 minutes after 5 minutes of 0.6% acetic acid injection (D).

Table 5: Effect of chalcone derivatives on acetic acid induced writhing

Treatment Group	Drug dose mg/kg	Number of writhing	% Inhibition
Control (1% CMC)	1ml	101.0±3.5	0.0
DS	20	62.0±9.0	38.6
3a	20	73.0±5.5	27.7
3b	20	62.0±4.0	38.6
3c	20	47.0±2.0	53.5
3e	20	75.0±3.0	25.7

Table 6: Effect of chalcone derivatives on acetic acid induced licking

Treatment Group	Drug dose mg/kg	Number of lickings	% Inhibition
Control (1% CMC)	1ml	26.0±2.5	0.0
DS	20	8.0±1.0	69.2
3a	20	21.0±2.5	19.2
3b	20	22.0±3.5	15.3
3c	20	10.0±2.0	61.5
3e	20	18.0±1.5	30.8

3.4. Electronic properties of the compounds 3a-3e

All of the investigated compounds have shown evidence of the intra-molecular charge transfer (ICT) of the frontier molecular orbitals (FMOs) from highest occupied molecular orbitals (HOMOs) to lowest unoccupied molecular orbitals (LUMOs) (Figure 3). Findings in Table 7 demonstrate that the compounds (3a-3e) had greater E_{HOMO} levels than aspirin and lower E_{HOMO} values than trolox. HOMO-LUMO gaps (E_{gap}) of the studied compounds ranged from 3.6 eV (3a) to 3.9 eV (3a). All derivatives (3a-3e) have inferior E_{gap} than standard aspirin and trolox. Inferior E_{gap} means more reactivity, so the above said compounds are more reactive than aspirin and trolox. By removing electron from HOMO one-electron transfer radical cation can be gained. Ionization potential, IP is a key descriptor to evaluate range of electron transit. Smaller IP values and high electron affinities (EA) of the substances enlighten that compounds might show more promising electron transfer mechanism for the scavenging of free radicals [38]. The present analysis where tested compounds (3a-3e) also depicted low IP and higher EA values when compared with aspirin.

Table 7: Different HOMO energies (EHOMO), LUMO energies (ELUMO), HOMO-LUMO gaps (Egap), ionization potentials (IP) and electron affinities (EA) in eV of compounds **(3a-3e)** obtained at B3LYP/6-31G** level of theory.

Compounds	E_{HOMO}	E_{LUMO}	E_{gap}	**IP**	**EA**
Aspirin	-7.0	-1.5	5.5	7.0	1.5
Trolox	-5.4	0.1	5.5	5.4	-0.1
3a	-6.7	-2.8	3.9	6.7	2.8
3b	-6.8	-2.9	3.8	6.8	2.9
3c	-6.7	-2.9	3.8	6.7	2.9
3d	-6.5	-2.7	3.8	6.5	2.7
3e	-6.2	-2.6	3.6	6.2	2.6

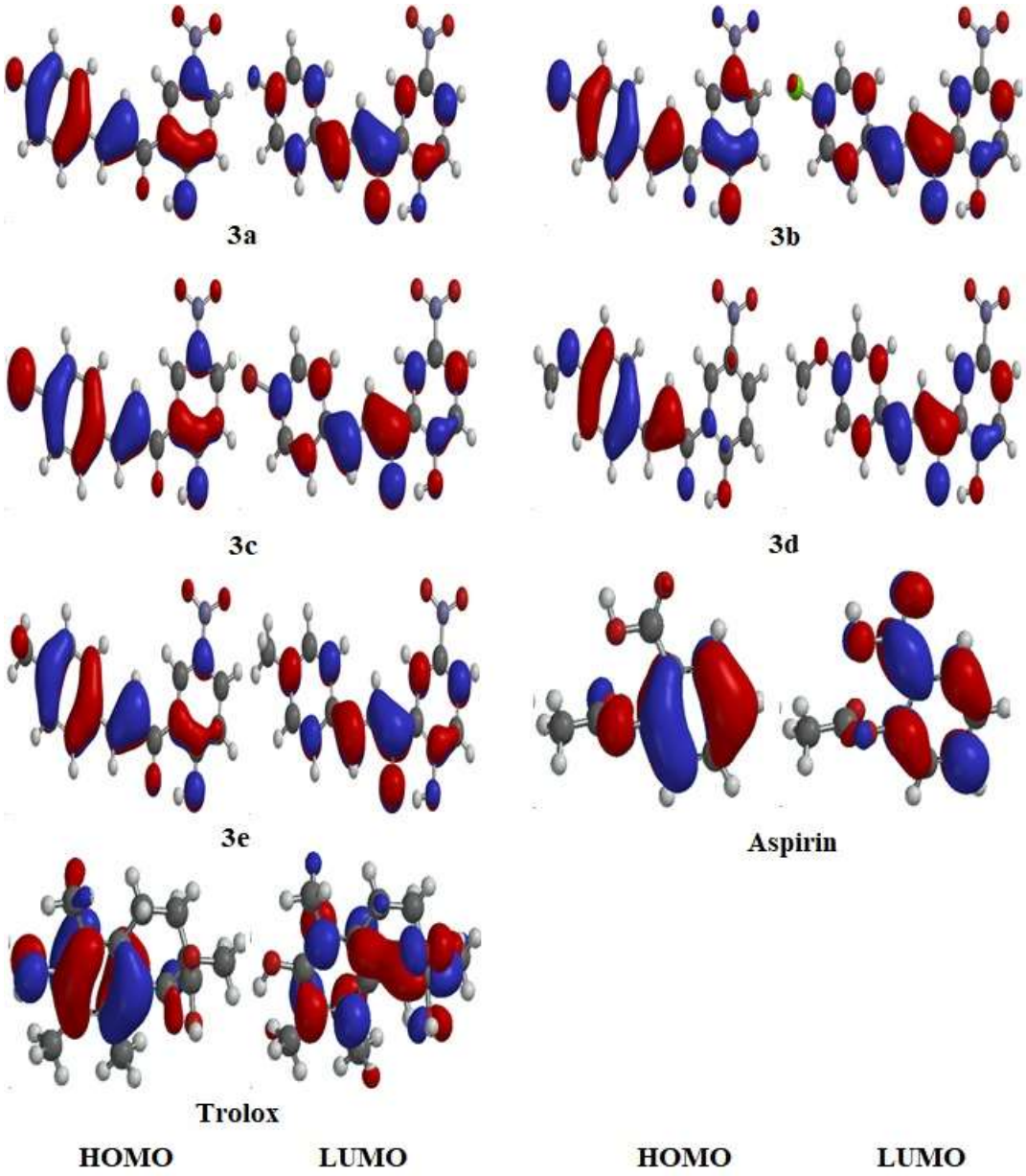

Figure 3: The distribution pattern of the HOMOs and LUMOs of the compounds **3a-3e** at ground states.

3.5. Molecular electrostatic potential (MEP) of compounds 3a-3e

MEP provides a link between molecular structure and physical properties of a compound. The term MEP refers to a quantitative description of a molecule's size, structure, and dipole moments as well as its electric potential. The reactive sites of molecules can therefore be deduced from this

map of the MEP surface [39]. This map can be used as a pointer to show which parts of a molecule are susceptible to an electrophilic and nucleophilic are attack [40]. MEP surface maps of the compounds **3a-3e** using Spartan '14 v1.1.8' at B3LYP/6-31G** level is calculated to understand the positive and negative MEP regions (Figure 4). The reactive sites are identified by various color codes and are very useful for exploring the relationship between the molecular structure and its physiochemical properties. In our studied compounds (**3a-3e**) positive potential was found on –OH groups colored red while the negative potential on keto oxygen colored blue. It is anticipated that favorable sites for electrophilic and nucleophilic attack would be keto groups and –OH, respectively.

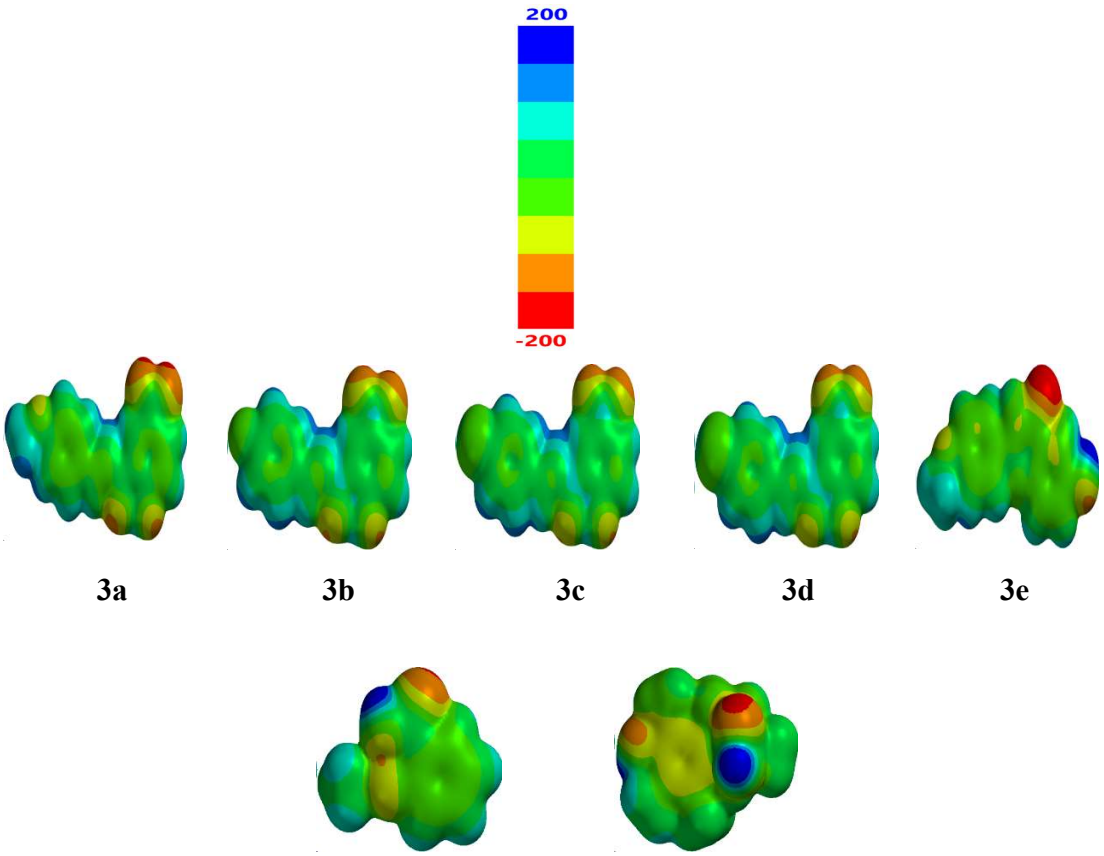

Figure 4: The molecular electrostatic potential of the compounds **3a-3e**

3.6. QSAR descriptors of compounds 3a-3e

Different QSAR descriptors of studied compounds obtained at B3LYP/6-31G** level of theory is summarized in Table 8. Partition coefficient (logP) is important descriptor for the lipophilicity of the compounds. All the studied compounds have negative logP values revealing that these compounds might be hydrophilic in nature. Furthermore, all the compounds are polar and have high solvation energies compared to standard aspirin and trolox. Polar surface area (PSA) is an important descriptor for drug permeability. For oral absorption and brain penetration of medications that are delivered through the transcellular channel, the polar surface area is the primary determinant. It has been demonstrated in previous research that PSA shouldn't be more than 120 A^2 for drugs that are taken orally and delivered by the transcellular route and <100 A^2 for brain penetration or <60-70 A^2 [41, 42]. In our compounds, the PSA of all the compounds is also less than 100 A^2 suggesting that they might have good absorption in the body. "According to rule of five" [43] the studied compounds are good drug candidates with molecular weight > 500, number of hydrogen bond donors (HBD) > 5, number of hydrogen bond acceptors (HBA) > 10 and logP > 5.

Table 8: QSAR descriptors (dipole moment= μD, area= A^2, volume= A^3, partition coefficient= LogP, hydrogen bond donor= HBD, hydrogen bond acceptor= HBA, polarizability= Pol., polar surface area= PSA and solvation energy= S.E. of compounds (**3a-3e**) obtained at B3LYP/6–31G** level of theory.

Compounds	**μD (Debye)**	**Area (A^2)**	**Volume (A^3)**	**Log P**	**HBD**	**HBA**	**Pol.**	**PSA (A^2)**	**S.E. (KJ/mol)**
Aspirin	2.7	196.4	174.9	1.2	1	7	54.3	52.0	-33.0
Trolox	2.9	275.2	264.3	4.3	2	2	61.5	49.9	-34.8

3a	2.0	287.1	267.8	-1.1	1	5	62.2	66.2	-160.3
3b	2.7	297.1	276.9	-0.7	1	5	62.9	66.2	-164.4
3c	2.1	301.8	381.5	-0.5	1	5	63.3	66.2	-166.6
3d	3.8	311.2	290.3	-1.6	1	6	64.1	66.2	-170.7
3e	2.8	301.4	281.5	-0.4	1	5	63.3	66.2	-163.5

4. Conclusion

New derivatives of chalcones were synthesized and characterized by spectroscopic studies. The synthesized compounds showed iron chelation, whilst QASR studies indicated they possessed a hydrophilic nature. Molecular docking study showed that these compounds possessed affinity with Keap1, that would favour the activation of Nrf2. Consequently, these compounds compare to several other studies exploring the capacity for chalcones to activate the Nrf2/Keap1 pathway through their capacity to sequester Keap1. Several studies have previously reported anti-inflammatory properties of alternative chalcone formulations *in vivo* [44]. In this study we identify that the newly characterized chalcones 3a and 3b possessed marked efficacy in vivo where they suppressed disease activity and pain in the carrageenan induced model of paw inflammation.

These studies suggest that these new 2-Hydroxy-5-nitro chalcones are potential anti-oxidant and anti-inflammatory compounds through their interaction with the Nrf2-Keap1 pathway. Further study of these compounds at the molecular level is now required to validate the presence of an Nrf2 dependent anti-inflammatory pathway. These compounds merit further be studied at molecular level to investigate their anti-inflammatory potential.

Acknowledgements

This work is supported by the Higher Education Commission of Pakistan and the School of Chemistry, University of the Punjab, Pakistan. "A. Irfan would like to acknowledge the King Khalid University through RCAMS/KKU/008-22 under the (Research Center for Advanced Materials Science) at King Khalid University, Kingdom of Saudi Arabia)."

Conflict of Interest

The authors declare that they have no conflict of interest.

References

1. Suzuki, K., *Chronic inflammation as an immunological abnormality and effectiveness of exercise.* Biomolecules, 2019. **9**(6): p. 223.
2. Bauer, M.E. and A.L. Teixeira, *Inflammation in psychiatric disorders: what comes first?* Annals of the New York Academy of Sciences, 2019.
3. Okamoto, N., et al., *Comparison of psychiatric symptoms between patients with major depression with higher and lower levels of high-sensitivity C-reactive protein in the serum: a preliminary study.* Therapeutic Advances in Psychopharmacology, 2021. **11**: p. 20451253211060228.
4. Soysal, P., et al., *Inflammation, frailty and cardiovascular disease.* Frailty and Cardiovascular Diseases, 2020: p. 55-64.
5. Kay, J., et al., *Inflammation-induced DNA damage, mutations and cancer.* DNA repair, 2019. **83**: p. 102673.
6. Ahmed, S.M.U., et al., *Nrf2 signaling pathway: Pivotal roles in inflammation.* Biochimica et Biophysica Acta (BBA)-Molecular Basis of Disease, 2017. **1863**(2): p. 585-597.
7. Sharma, S., et al., *Recent advancements in the development of heterocyclic anti-inflammatory agents.* European Journal of Medicinal Chemistry, 2020. **200**: p. 112438.
8. Kobayashi, M. and M. Yamamoto, *Molecular mechanisms activating the Nrf2-Keap1 pathway of antioxidant gene regulation.* Antioxidants & redox signaling, 2005. **7**(3-4): p. 385-394.
9. Mahapatra, D.K., S.K. Bharti, and V. Asati, *Anti-cancer chalcones: Structural and molecular target perspectives.* European journal of medicinal chemistry, 2015. **98**: p. 69-114.
10. Cazarolli, L.H., et al., *Natural and synthetic chalcones: tools for the study of targets of action—insulin secretagogue or insulin mimetic?* Studies in natural products chemistry, 2013. **39**: p. 47-89.
11. ur Rashid, H., et al., *Promising anti-inflammatory effects of chalcones via inhibition of cyclooxygenase, prostaglandin E2, inducible NO synthase and nuclear factor κb activities.* Bioorganic Chemistry, 2019. **87**: p. 335-365.

12. J Leon-Gonzalez, A., et al., *Chalcones as promising lead compounds on cancer therapy.* Current medicinal chemistry, 2015. **22**(30): p. 3407-3425.
13. Xu, M., et al., *Chalcone derivatives and their antibacterial activities: Current development.* Bioorganic chemistry, 2019. **91**: p. 103133.
14. Yadav, N., et al., *Antimalarial activity of newly synthesized chalcone derivatives in vitro.* Chemical biology & drug design, 2012. **80**(2): p. 340-347.
15. Cheenpracha, S., et al., *Anti-HIV-1 protease activity of compounds from Boesenbergia pandurata.* Bioorganic & medicinal chemistry, 2006. **14**(6): p. 1710-1714.
16. de Mello, M.V.P., et al., *A comprehensive review of chalcone derivatives as antileishmanial agents.* European journal of medicinal chemistry, 2018. **150**: p. 920-929.
17. Rampa, A., et al., *Exploiting the chalcone scaffold to develop multifunctional agents for Alzheimer's disease.* Molecules, 2018. **23**(8): p. 1902.
18. Adelusi, T.I., et al., *Neurotrophic, anti-neuroinflammatory, and redox balance mechanisms of chalcones.* European Journal of Pharmacology, 2021. **891**: p. 173695.
19. Kim, S., et al., *Nrf2 activator via interference of Nrf2-Keap1 interaction has antioxidant and anti-inflammatory properties in Parkinson's disease animal model.* Neuropharmacology, 2020. **167**: p. 107989.
20. Siddiqa, A., et al., *Synthesis, antioxidant, in silico and computational investigation of 2, 5-dihydroxyacetophenone derived chloro-substituted hydroxychalcones, hydroxyflavanones and hydroxyflavindogenides.* Journal of Biomolecular Structure and Dynamics, 2021: p. 1-13.
21. Tajammal, A., et al., *Synthesis, antihyperglycemic activity and computational studies of antioxidant chalcones and flavanones derived from 2, 5 dihydroxyacetophenone.* Journal of Molecular Structure, 2017. **1148**: p. 512-520.
22. Athar, M., et al., *Pharmacophore model prediction, 3D-QSAR and molecular docking studies on vinyl sulfones targeting Nrf2-mediated gene transcription intended for anti-Parkinson drug design.* Journal of Biomolecular Structure and Dynamics, 2016. **34**(6): p. 1282-1297.
23. Schneidman-Duhovny, D., et al., *PatchDock and SymmDock: servers for rigid and symmetric docking.* Nucleic acids research, 2005. **33**(suppl_2): p. W363-W367.
24. Samra, M.M., et al., *Synthesis, characterization, docking and biological studies of M (II)(M= Mg, Ca, Sr) Piroxicam complexes.* Journal of Molecular Structure, 2022. **1254**: p. 132256.
25. Hoonur, R.S., et al., *Transition metal complexes of 3-aryl-2-substituted 1, 2-dihydroquinazolin-4 (3H)-one derivatives: New class of analgesic and anti-inflammatory agents.* European journal of medicinal chemistry, 2010. **45**(6): p. 2277-2282.
26. Belcastro, M., et al., *Structural and electronic characterization of antioxidants from marine organisms.* Theoretical Chemistry Accounts, 2006. **115**(5): p. 361-369.
27. Wright, J.S., E.R. Johnson, and G.A. DiLabio, *Predicting the activity of phenolic antioxidants: theoretical method, analysis of substituent effects, and application to major families of antioxidants.* Journal of the American Chemical Society, 2001. **123**(6): p. 1173-1183.
28. Irfan, A. and A.G. Al-Sehemi, *DFT study of the electronic and charge transfer properties of perfluoroarene–thiophene oligomers.* Journal of Saudi Chemical Society, 2014. **18**(5): p. 574-580.

29. Chaudhry, A.R., et al., *Effect of heteroatoms substitution on electronic, photophysical and charge transfer properties of naphtha [2, 1-b: 6, 5-b'] difuran analogues by density functional theory.* Computational and Theoretical Chemistry, 2014. **1045**: p. 123-134.
30. Chaudhry, A.R., et al., *First Principles Investigations of Electronic, Photoluminescence and Charge Transfer Properties of the Naphtho [2, 1-b: 6, 5-b'] difuran and Its Derivatives for OFET.* Sains Malaysiana, 2014. **43**(6): p. 867-875.
31. Irfan, A., et al., *Electro-optical, nonlinear and charge transfer properties of naphthalene based compounds: a dual approach study.* Optik, 2017. **132**: p. 101-110.
32. Irfan, A., et al., *The structural, electro-optical, charge transport and nonlinear optical properties of 2-[(3, 5-dimethyl-1-phenyl-1H-pyrazol-4-yl) methylidene] indan-1, 3-dione.* Optik, 2016. **127**(21): p. 10148-10157.
33. Al-Sehemi, A.G., et al., *Density functional theory investigations of radical scavenging activity of 3'-Methyl-quercetin.* Journal of Saudi Chemical Society, 2016. **20**: p. S21-S28.
34. Al-Sehemi, A.G., et al., *Computational study and in vitro evaluation of the anti-proliferative activity of novel naproxen derivatives.* Journal of King Saud University-Science, 2017. **29**(3): p. 311-319.
35. Al-Sehemi, A.G., et al., *Antibacterial activities, DFT and QSAR studies of quinazolinone compounds.* Bulletin of the Chemical Society of Ethiopia, 2016. **30**(2): p. 307-316.
36. Li, M., et al., *Discovery of Keap1− Nrf2 small− molecule inhibitors from phytochemicals based on molecular docking.* Food and Chemical Toxicology, 2019. **133**: p. 110758.
37. Lakshminarayanan, B., N. Kannappan, and T. Subburaju, *SYNTHESIS AND BIOLOGICAL EVALUATION OF NOVEL CHALCONES WITH METHANE-SULFONYL END AS POTENT ANALGESIC AND ANTI-INFLAMMATORY AGENTS.*
38. Tajammal, A., et al., *Antioxidant, molecular docking and computational investigation of new flavonoids.* Journal of Molecular Structure, 2022. **1254**: p. 132189.
39. Scrocco, E. and J. Tomasi, *Electronic molecular structure, reactivity and intermolecular forces: an euristic interpretation by means of electrostatic molecular potentials*, in *Advances in quantum chemistry*. 1978, Elsevier. p. 115-193.
40. Swarnalatha, N., et al., *Vibrational, UV spectra, NBO, first order hyperpolarizability and HOMO–LUMO analysis of carvedilol.* Spectrochimica Acta Part A: Molecular and Biomolecular Spectroscopy, 2015. **136**: p. 567-578.
41. van de Waterbeemd, H., et al., *Estimation of blood-brain barrier crossing of drugs using molecular size and shape, and H-bonding descriptors.* Journal of drug targeting, 1998. **6**(2): p. 151-165.
42. Kelder, J., et al., *Polar molecular surface as a dominating determinant for oral absorption and brain penetration of drugs.* Pharmaceutical research, 1999. **16**(10): p. 1514-1519.
43. Clark, D.E., *Rapid calculation of polar molecular surface area and its application to the prediction of transport phenomena. 1. Prediction of intestinal absorption.* Journal of pharmaceutical sciences, 1999. **88**(8): p. 807-814.
44. Emam, S.H., et al., *Design and synthesis of methoxyphenyl-and coumarin-based chalcone derivatives as anti-inflammatory agents by inhibition of NO production and down-regulation of NF-κB in LPS-induced RAW264. 7 macrophage cells.* Bioorganic Chemistry, 2021. **107**: p. 104630.

Supplementary Data

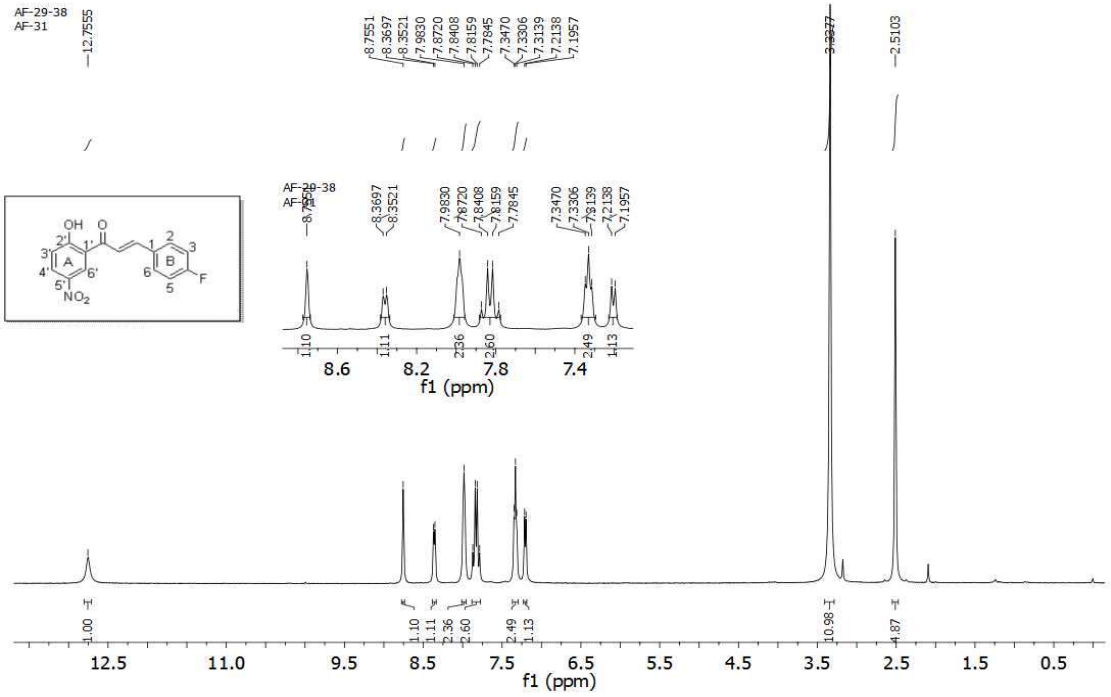

Figure S1: ^{1}H NMR of 3a

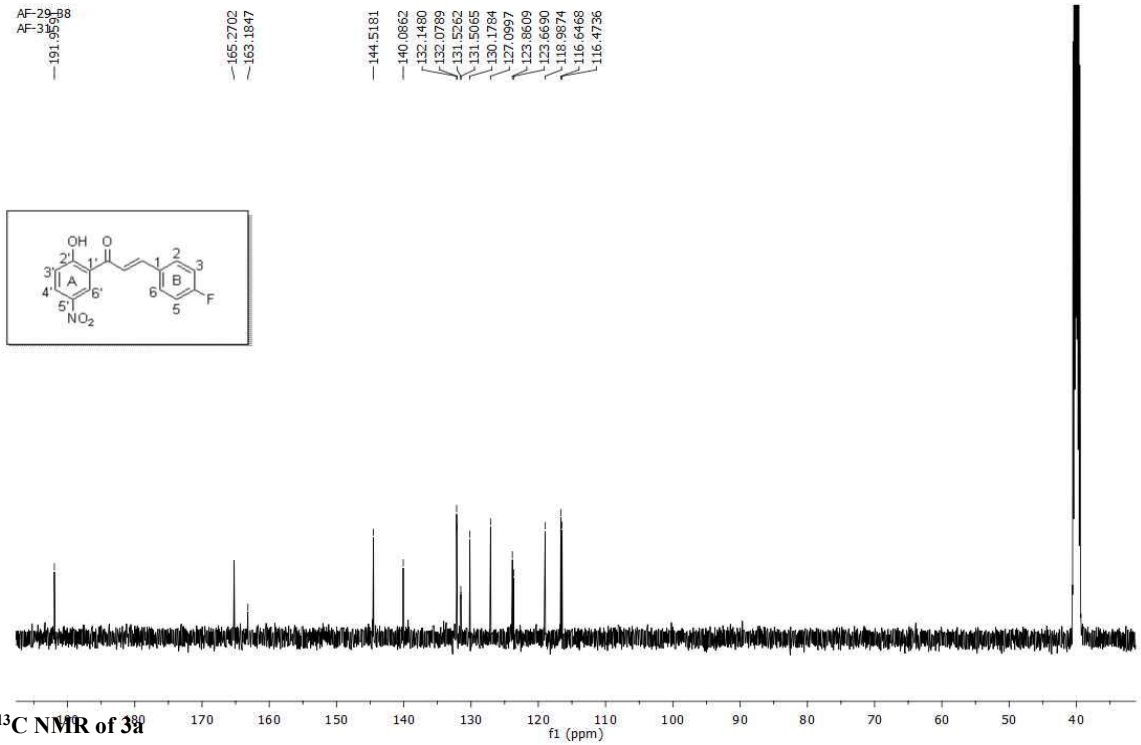

Figure S2: ^{13}C NMR of 3a

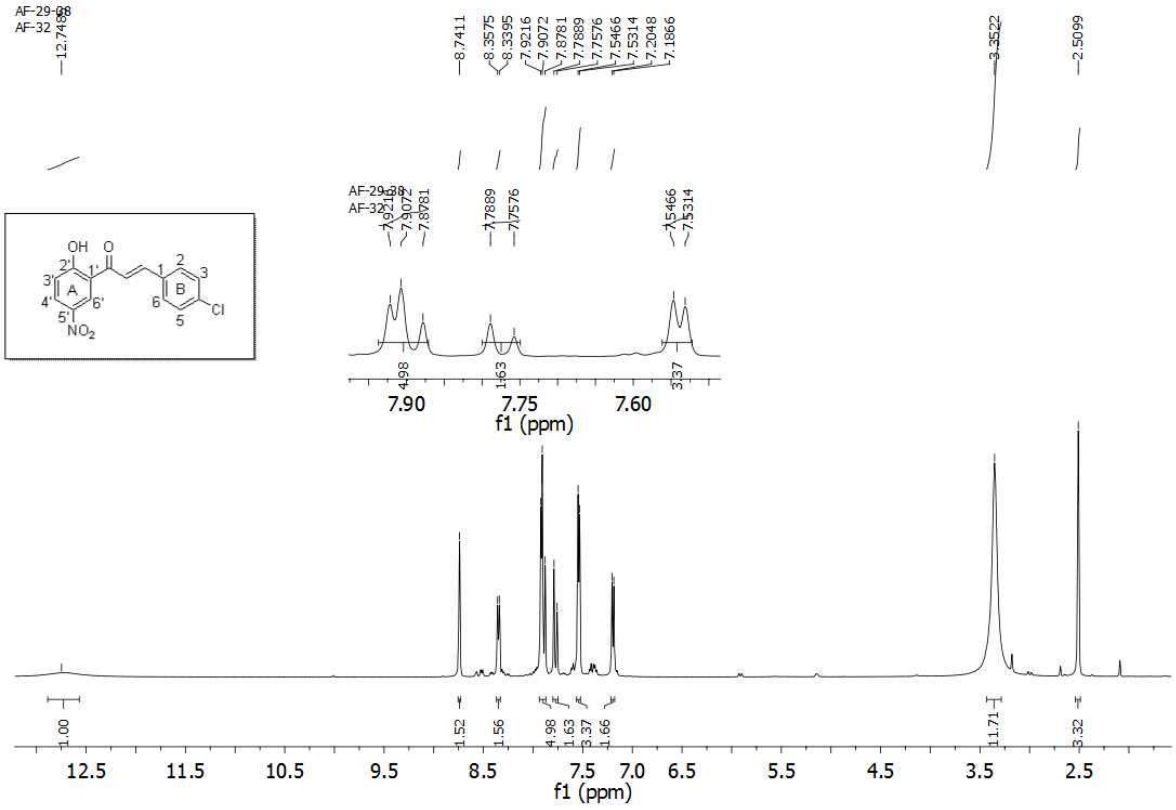

Figure S3: ^{1}H NMR of 3b

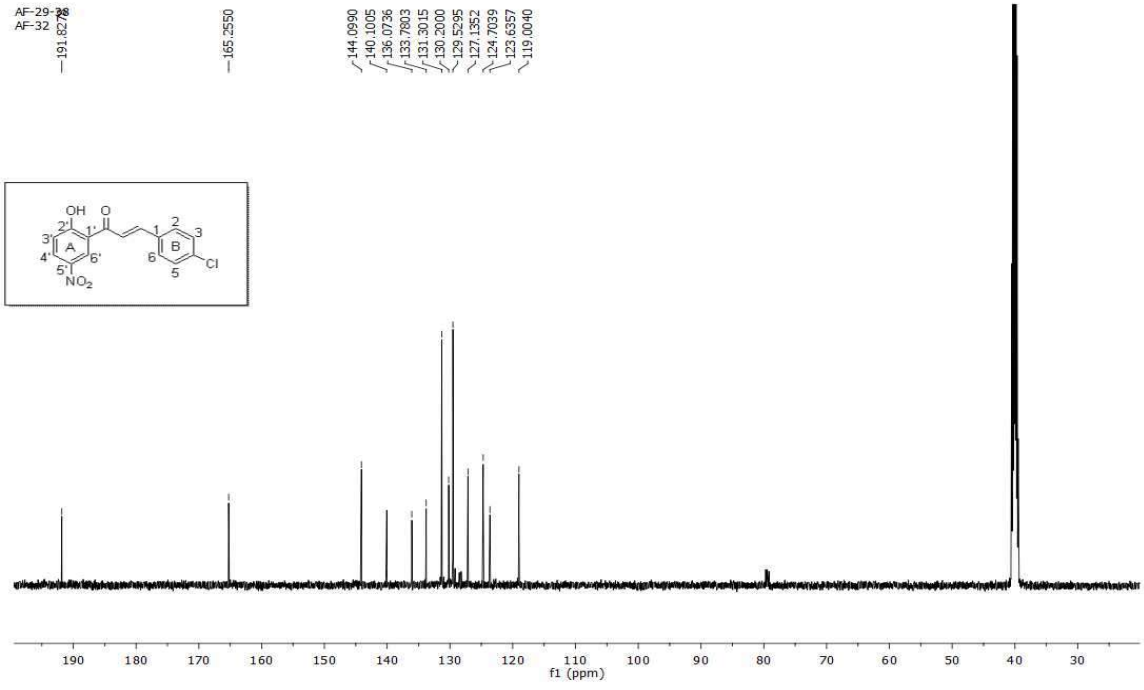

Figure S4: ^{13}C NMR of 3b

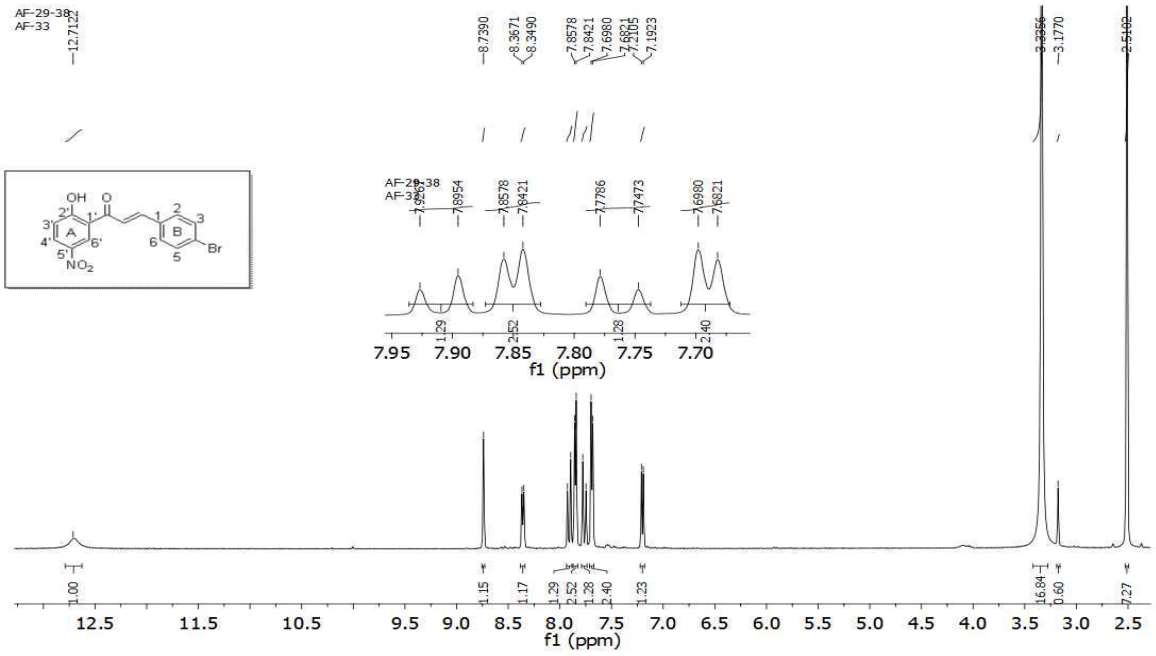

Figure S5: ^{1}H NMR of 3c

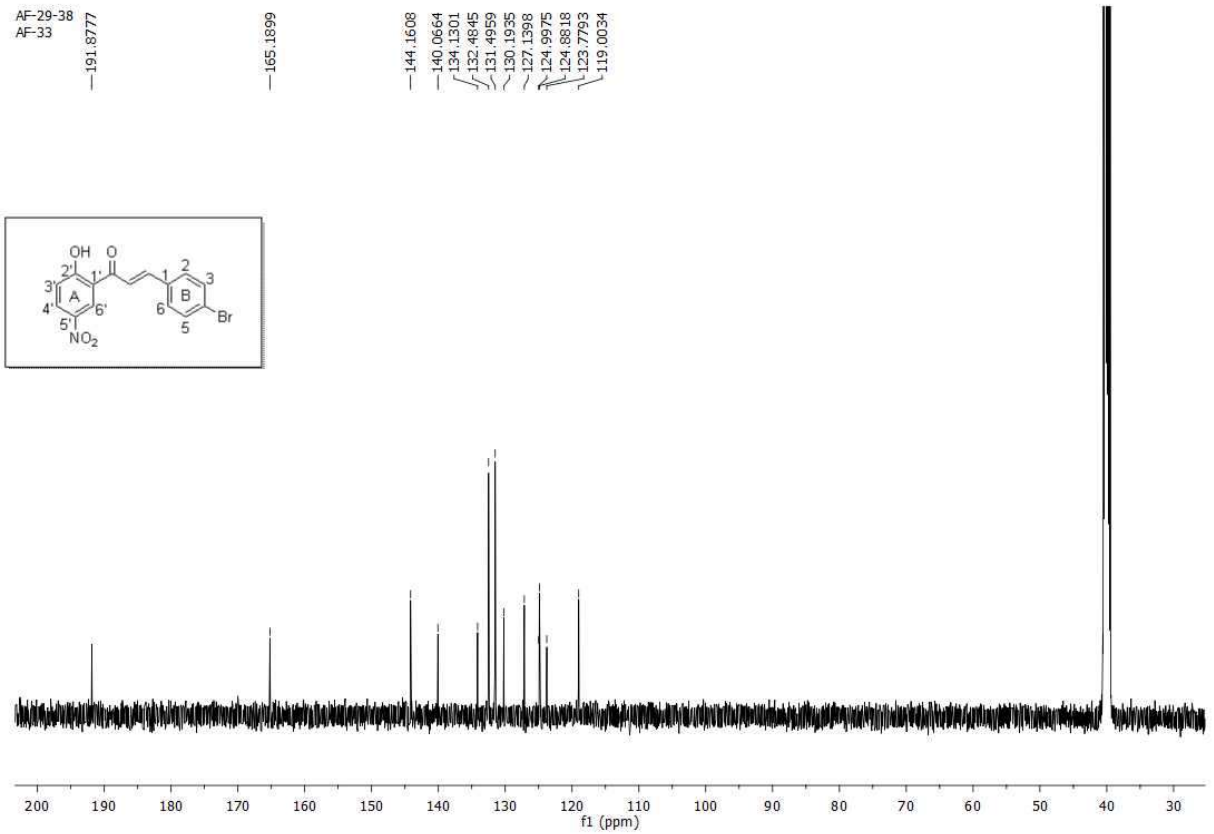

Figure S6: ^{13}C NMR of 3c

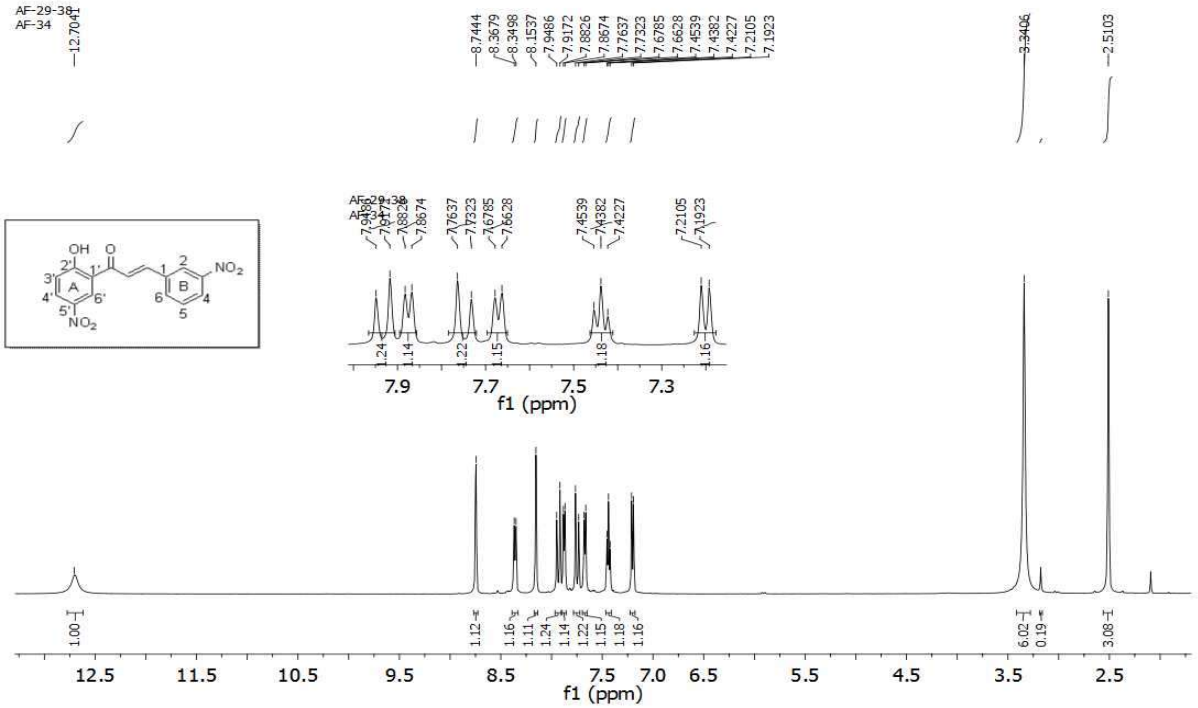

Figure S7: ^{1}H NMR of 3d

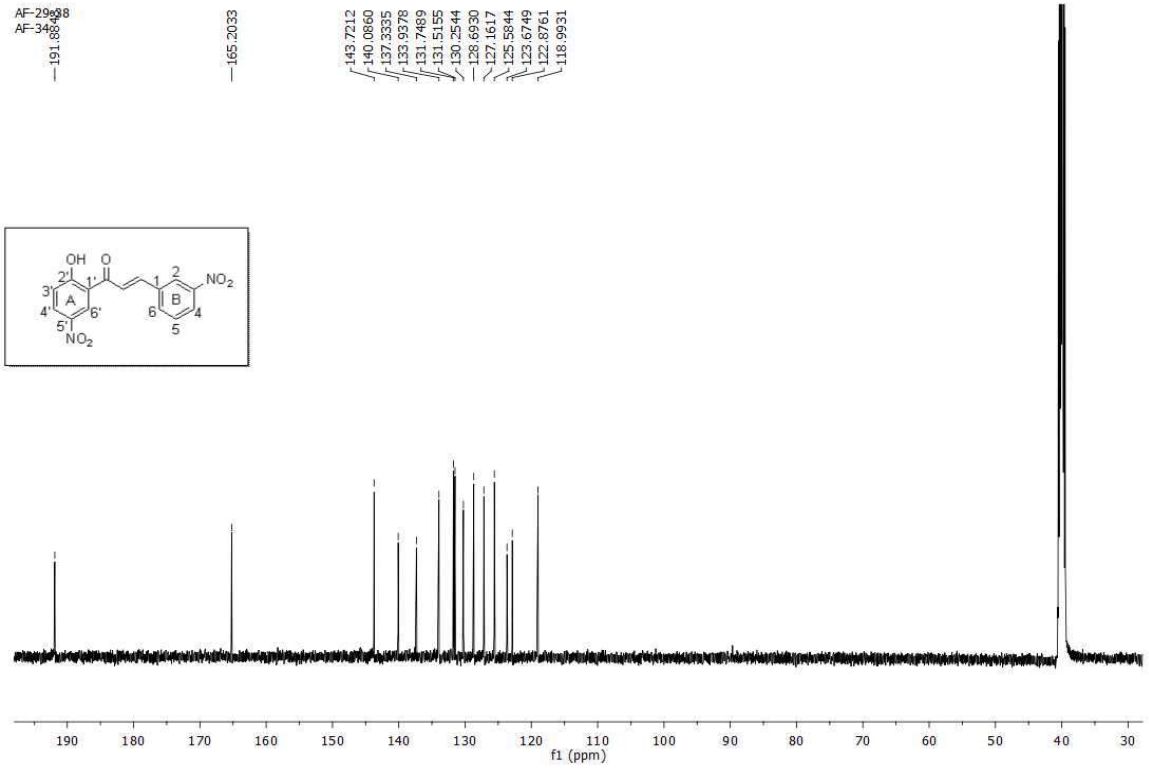

Figure S8: ^{13}C NMR of 3d

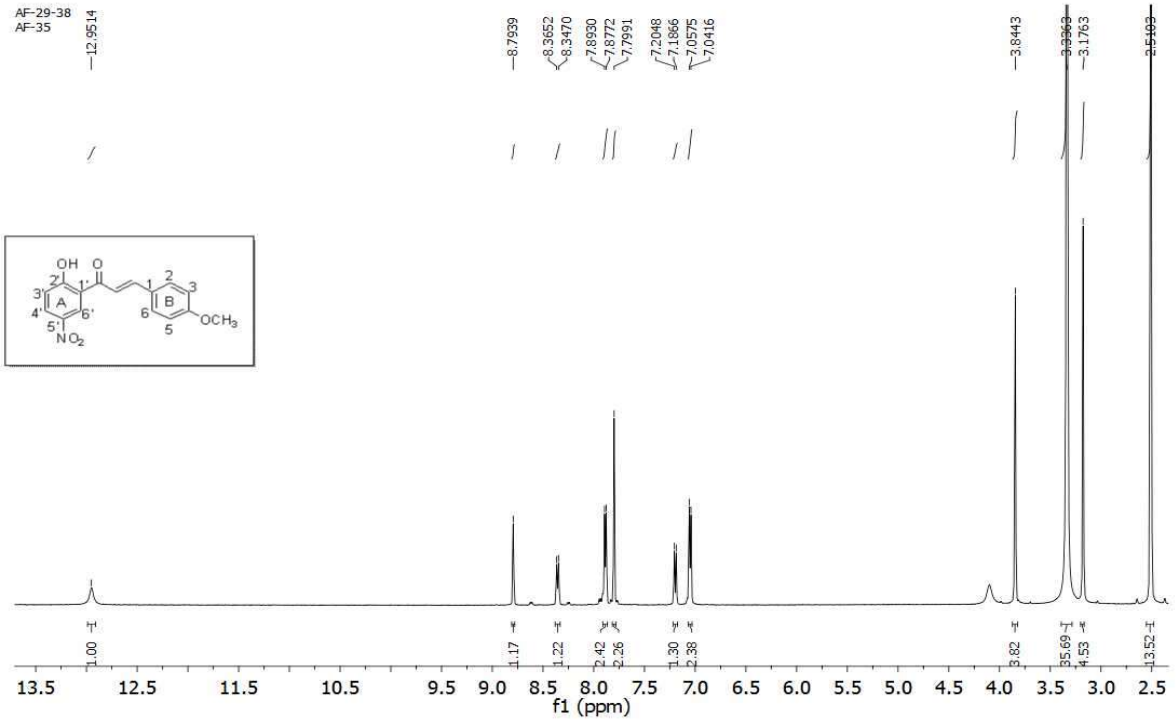

Figure S9: ^{1}H NMR of 3e

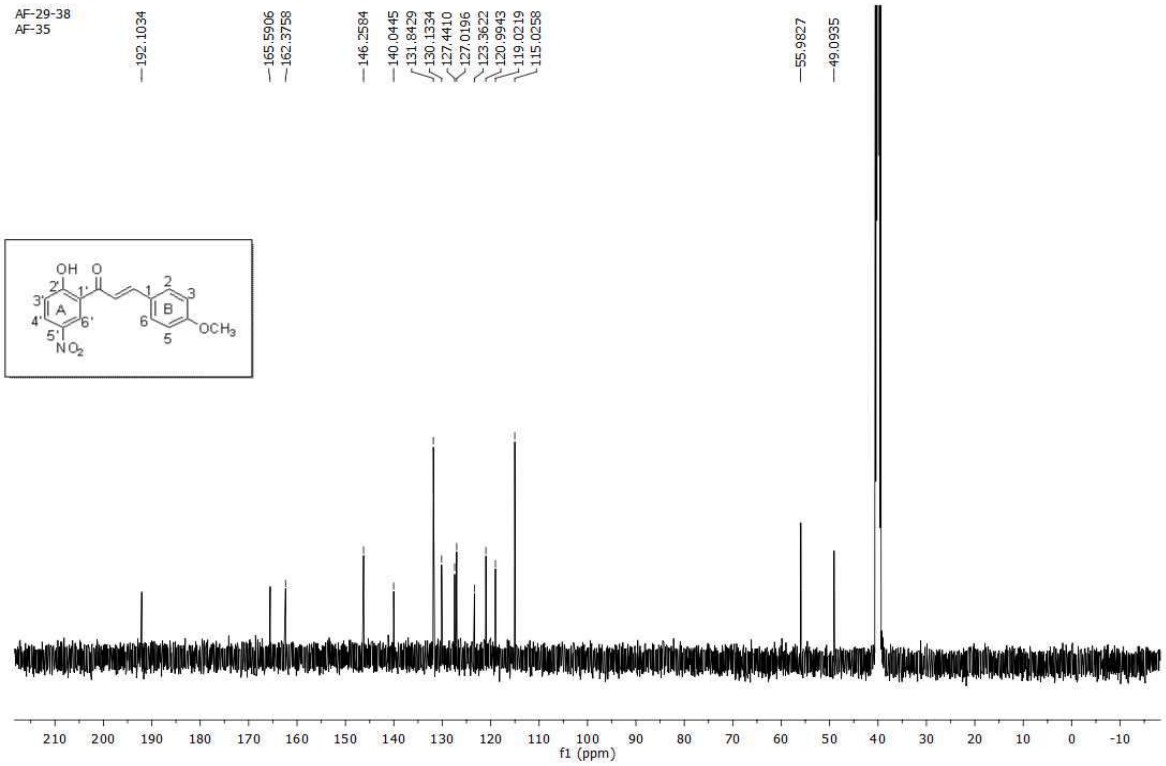

Figure S10: ^{13}C NMR of 3e

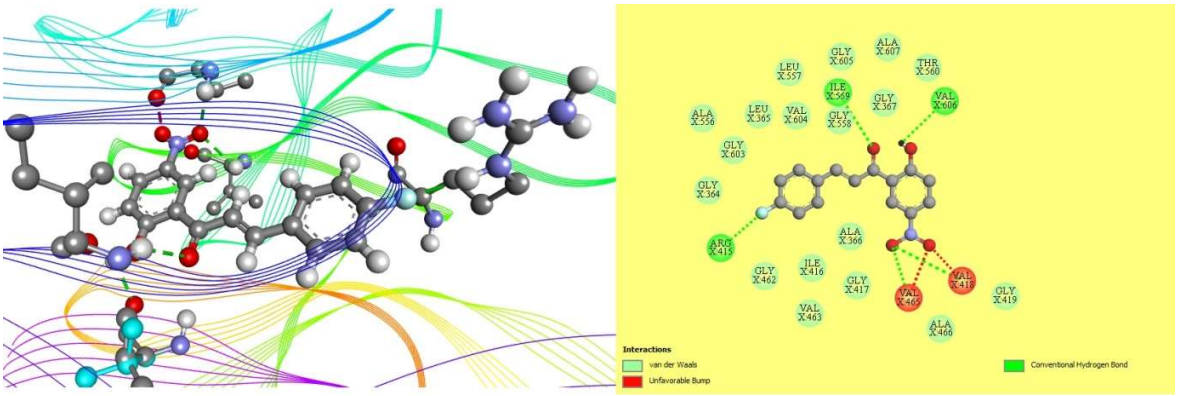

Figure S11: Illustration of 3D (A) and 2D (B) molecular interactions of 3a with Keap1

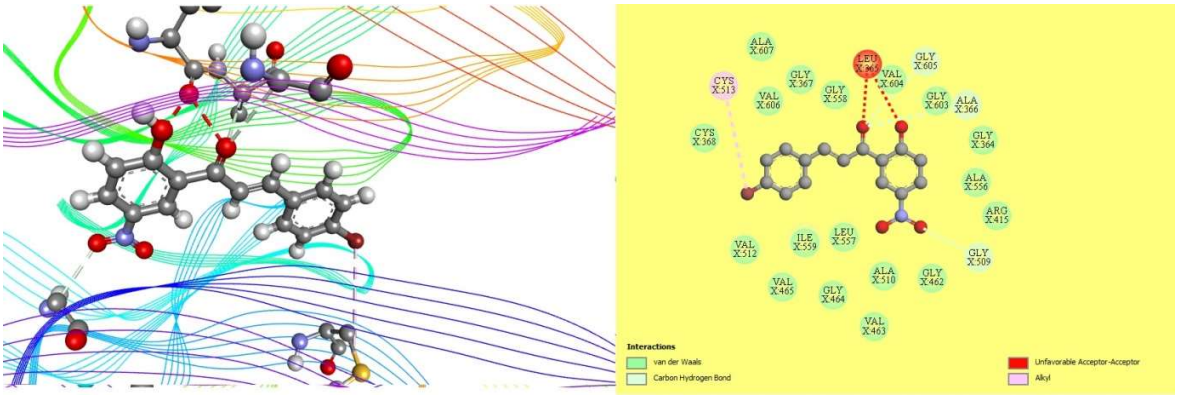

Figure S12: Illustration of 3D (A) and 2D (B) molecular interactions of 3c with Keap1

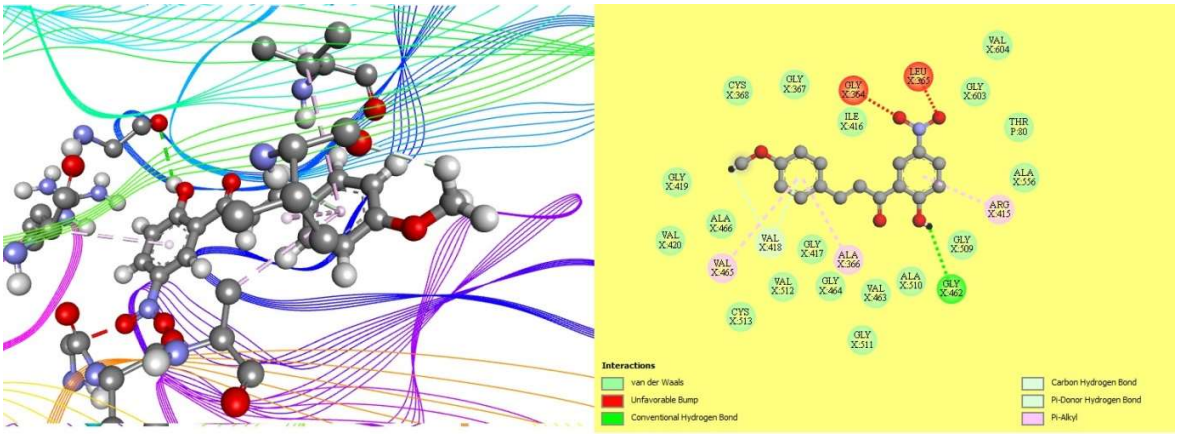

Figure S13: Illustration of 3D (A) and 2D (B) molecular interactions of 3d with Keap1

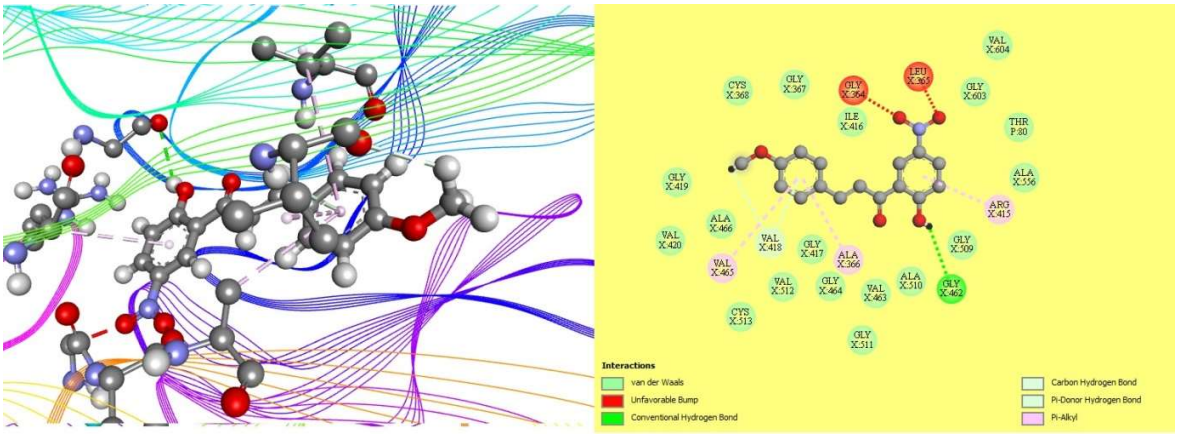

Figure S14: Illustration of 3D (A) and 2D (B) molecular interactions of 3e with Keap1

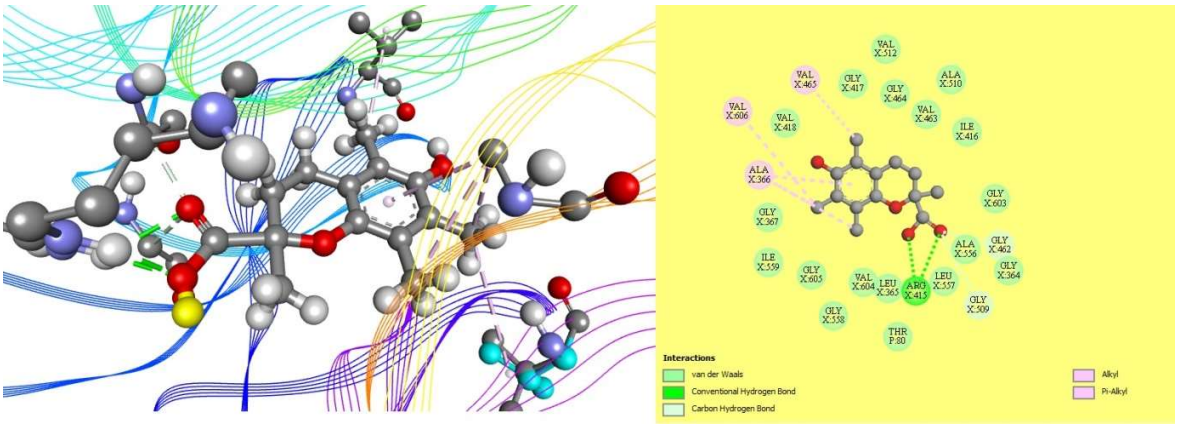

Figure S15: Illustration of 3D (A) and 2D (B) molecular interactions of ascorbic acid with Keap1

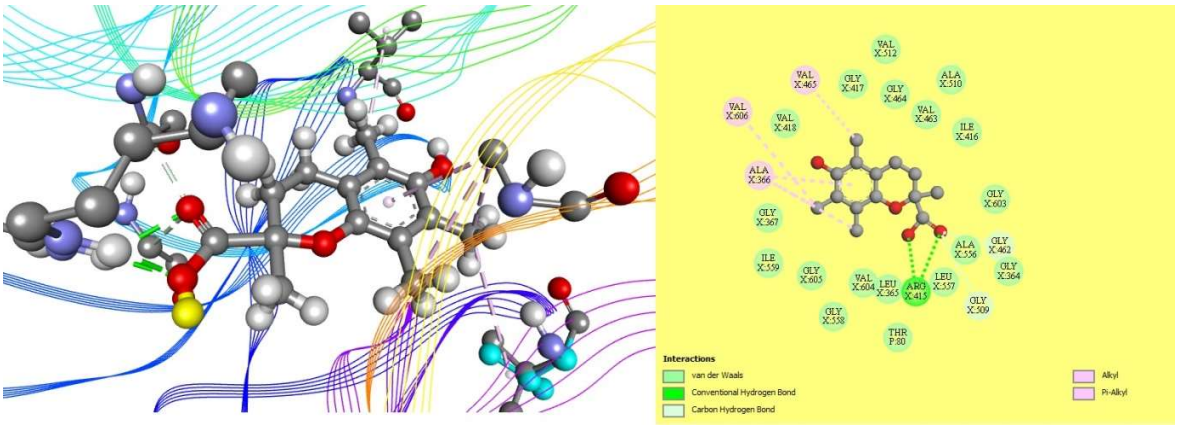

Figure S16: Illustration of 3D (A) and 2D (B) molecular interactions of trolox with Keap1